Supplemental Information

Menin inhibitor MI-3454 induces remission in *MLL1*-rearranged and *NPM1*-mutated models of leukemia

Szymon Klossowski[1,11], Hongzhi Miao[1,11], Katarzyna Kempinska[1,11], Tao Wu[2], Trupta Purohit[1], EunGi Kim[1], Brian M. Linhares[1], Dong Chen[1], Gloria Jih[3], Eric Perkey[3], Huang Huang[1], Miao He[4], Bo Wen[4], Yi Wang[2], Ke Yu[2], Stanley Chun-Wei Lee[5], Gwenn Danet-Desnoyers[6], Winifred Trotman[6], Malathi Kandarpa[7], Anitria Cotton[8], Omar Abdel-Wahab[5], Hongwei Lei[1], Yali Dou[1], Monica Guzman[9], Luke Peterson[7], Tanja Gruber[8], Sarah Choi[1], Duxin Sun[4], Pingda Ren[2,10], Lian-Sheng Li[2], Yi Liu[2], Francis Burrows[10], Ivan Maillard[3,6], Tomasz Cierpicki[1]*, Jolanta Grembecka[1]*

[1]Department of Pathology; [3]Life Sciences Institute; [4]College of Pharmacy; [7]Department of Internal Medicine, Division of Hematology/Oncology, University of Michigan, Ann Arbor, MI, 48109,
[2]Wellspring Biosciences, Inc., San Diego, CA 92121
[5]Memorial Sloan Kettering Cancer Center, New York, NY 10065
[6]Division of Hematology-Oncology, Perelman School of Medicine, University of Pennsylvania, Philadelphia, PA, 19104
[8]St. Jude Children's Hospital, Memphis, TN, 38105
[9]Weill Cornell Medicine, New York, NY, 10065
[10]Kura Oncology, Inc., San Diego, CA 92121
[11]These authors contributed equally to this work

[*]Corresponding authors:
Jolanta Grembecka, PhD
Associate Professor, Department of Pathology, University of Michigan
1150 West Medical Center Dr, MSRB I, Room 4510D, Ann Arbor, MI, 48108
e-mail: jolantag@umich.edu, Tel. 734-615-9319
AND
Tomasz Cierpicki, PhD
Associate Professor, Department of Pathology, University of Michigan
1150 West Medical Center Dr, MSRB I, Room 4510C, Ann Arbor, MI, 48108
e-mail: tomaszc@umich.edu, Tel. 734-615-9324

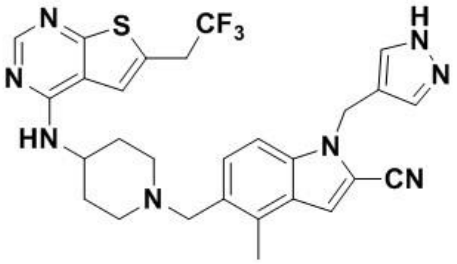

MI-503

$IC_{50\,(MLL4\text{-}43)} = 33 \pm 8.5$ nM

$K_d = 9.3$ nM

Supplemental Figure 1. Chemical structure and activity of MI-503 menin-MLL1 inhibitor (1, 2).

A

Mouse			Human		
$T_{1/2}$ (min)	CL-int (mL/min/kg)	CL-hep (mL/min/kg)	$T_{1/2}$ (min)	CL-int (mL/min/kg)	CL-hep (mL/min/kg)
20.4	458	75.2	37.1	59	14.9

B

% inhibition at 10 µM of MI-3454					
CYP-2D6	CYP-2C9	CYP-2C19	CYP-1A2	CYP-2C8	CYP-3A4
34	17	<10	48	46	76

C

Route	Dose (mg/kg)	C_{max} (ng/mL)	T_{max} (hr)	$AUC_{0\text{-tldc}}$ (hr*ng/mL)	$AUC_{0\text{-inf}}$ (hr*ng/mL)	$T_{1/2}$ (hr)	CL (mL/hr/kg)	CL/F (mL/hr/kg)	V_{ss} (mL/kg)	V_z/F (mL/kg)	%F (%)
i.v.	15	ND	ND	6298	6315	2.4	2375	ND	5358	NA	NA
p.o.	100	4698	2	32386	32631	3.2	ND	3065	ND	13955	77.5

D

Time point	MI-3454 (nM) in plasma	MI-3454 (nM) in brain	MI-3454 (nM) in CSF
3h	2403	81.8	35.9
7h	1436	44.9	2.7
24h	15.7	2.8	37.6

Supplemental Figure 2. Profiling of MI-3454. A. Microsomal stability of MI-3454 in murine and human mouse liver microsomes. $T_{1/2}$ – half life, CL-int - intestinal clearance, CL-hep - hepatic clearance. **B**. Inhibition of CYP-450 isoforms by MI-3454. **C**. PK parameters for MI-3454 upon i.v. and oral administration to CD-1 mice. Pharmacokinetic parameters: Cl (clearance), AUC (area under the curve), V_{ss} (volume of distribution at steady state), V_z (volume of distribution during terminal phase), F (bioavailability), C_{max} (maximum concentration achieved), T_{max} (time at which maximum concentration was achieved), were calculated by noncompartmental methods using WinNonlin® software version 3.2. NA – not applicable, ND – not determined. n = 3 mice / group. **D.** Level of MI-3454 in plasma, brain and cerebrospinal fluid (CSF) upon oral administration of 100 mg/kg of MI-3454 to CD-1 mice. n = 3-4 mice / group.

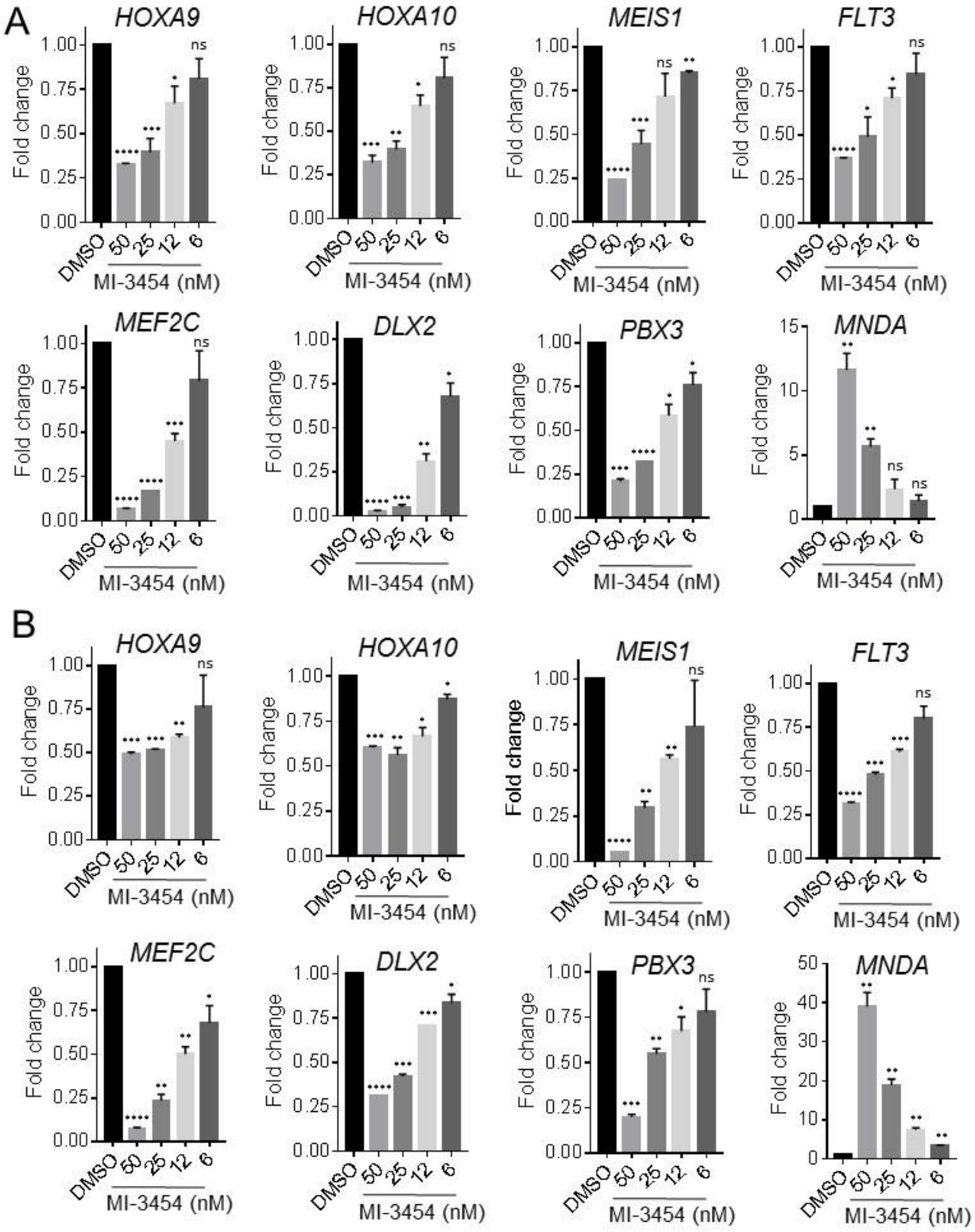

Supplemental Figure 3. Gene expression studies with MI-3454 in MLL leukemia cells. (A and **B).** Quantitative RT-PCR performed in MV4;11 cells (**A**) or MOLM13 cells (**B**) after 6 days of treatment with MI-3454. Gene expression was normalized to HPRT1 and referenced to the DMSO-treated cells. Data represent two independent experiments each performed in duplicates. Mean values for duplicates ± SD are shown. In panels A-B: *p<0.05, **p<0.01, ***p<0.001, ****p<0.0001, ns – not significant, calculated using Student's 2-tailed t-test.

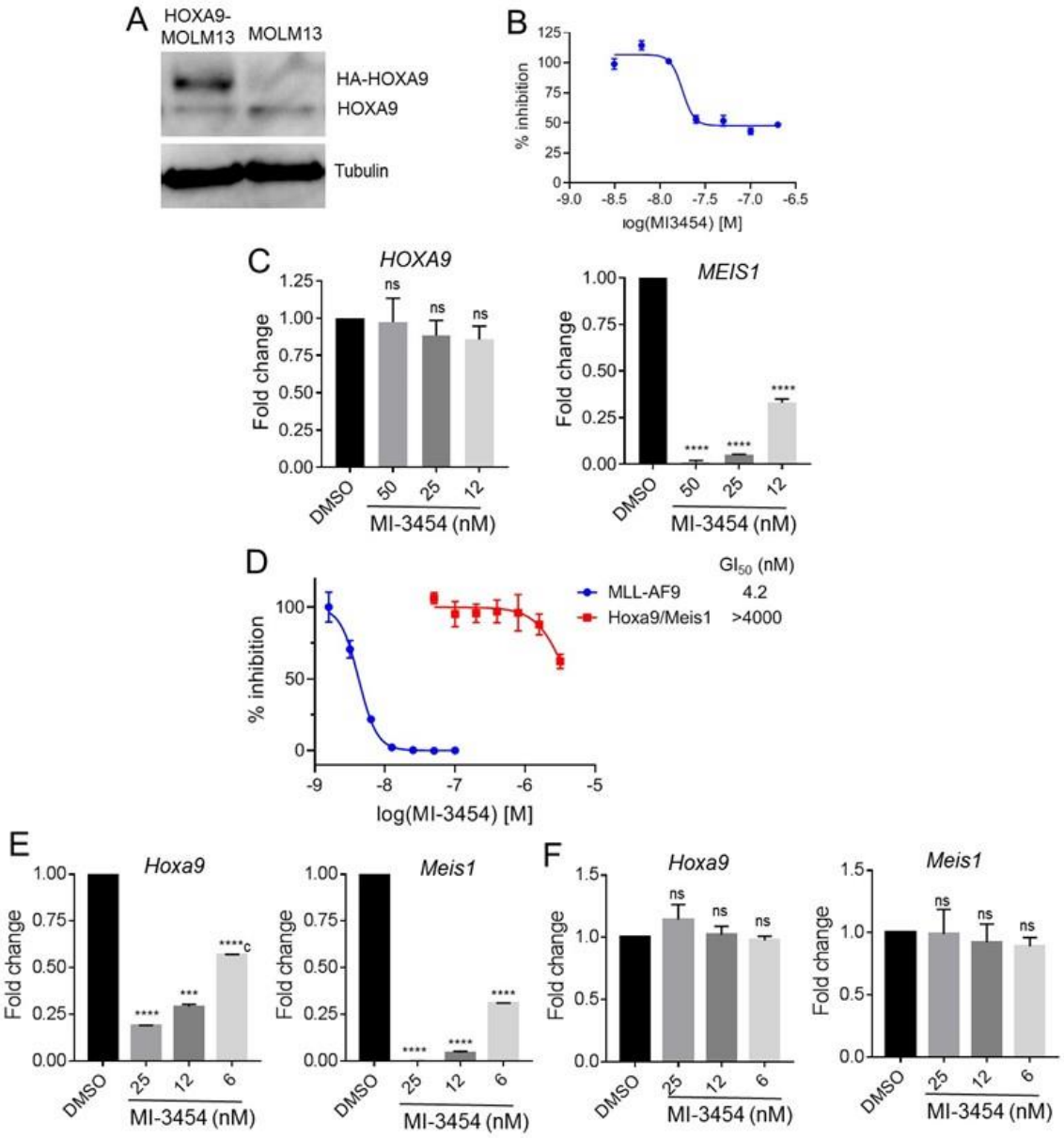

Supplemental Figure 4. Activity of MI-3454 in leukemia cells. A. Western Blot validating overexpression of *HOXA9* (*HA-HOXA9*) in MOLM13 cell line. Endogenous *HOXA* is marked as well. **B**. MTT cell viability assay for MI-3454 in MOLM13 cell line with overexpression of *HOXA9* (HOXA9-MOLM13). Only partial cell growth inhibition (up to ~50%) was observed upon 7 days of treatment with MI-3454 or DMSO. mean ± SD, n = 4. 2 independent MTT experiments were performed. **C**. Effect of MI-3454 on the expression level of *HOXA9* and *MEIS1* in HOXA9-MOLM13 cells. *HOXA9* is not affected by MI-3454 in these cells, while *MEIS1* expression is changed to a similar extent as in the parental MOLM13 cell line. Data represent two independent experiments each performed in triplicates, (mean ± SD, n = 3). **D.** MTT cell viability assay in murine bone marrow cells transformed with *MLL-AF9* or *Hoxa9/Meis1* after 7 days of treatment with MI-3454 or DMSO. mean ± SD, n = 4. 2 independent MTT experiments were performed. **E, F.** Gene expression studies with MI-3454 in murine bone marrow cells transformed with *MLL-AF9* (**E**) or *Hoxa9/Meis1* (**F**) oncogenes after 6 days of treatment. Data represent two independent experiments each performed in duplicates (**E**) or triplicates (**F**), (mean ± SD, n = 2-3). In panels **C**, **E**, **F**: ***p<0.001, ****p<0.0001, ns – not significant.

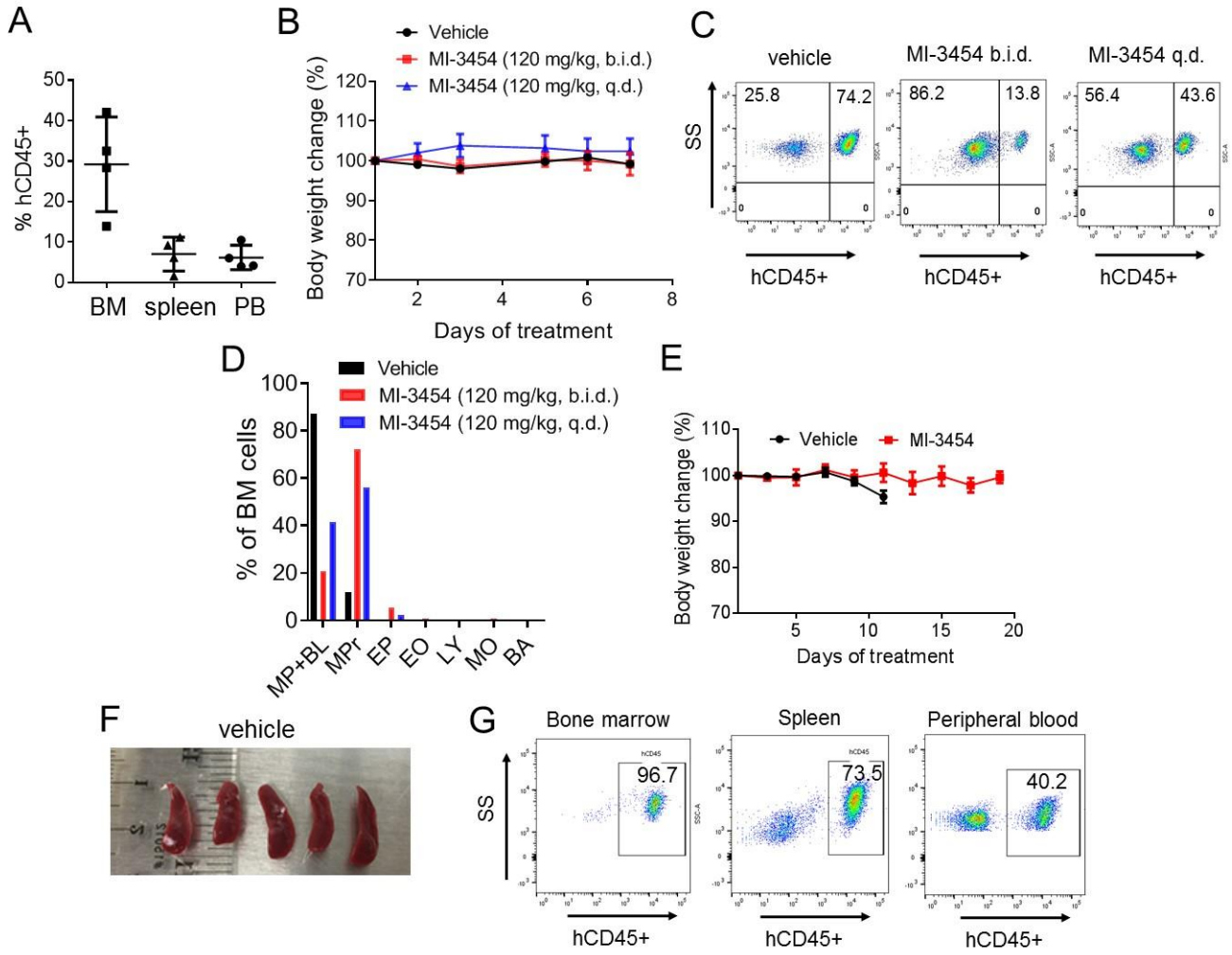

Supplemental Figure 5. ***In vivo*** **activity of MI-3454 in MLL leukemia models. A**. Flow cytometry analysis of the level of hCD45+ cells in bone marrow (BM), spleen and peripheral blood (PB) of mice transplanted with MV4;11 cells expressing luciferase performed at day 19 after transplantation. n = 4 mice / group, mean values +/- SD are shown. **B**. Body weight change of NSG mice transplanted with MV4;11 cells during seven days of treatment with MI-3454 or vehicle (mean ± SD, n = 5). Body weight measurements are reference to the values obtained at the first day of treatment, which were set as 100%. **C**. Representative flow cytometry histograms for quantification of hCD45+ cells in bone marrow samples of mice transplanted with MV4;11 cells after 7 days of treatment with MI-3454 (120 mg/kg. p.o.) or vehicle. SS – side scatter. **D**. Differential counting of cells in bone marrow cytospins of bone marrow (BM) samples collected from mice transplanted with MV4;11 cells after 7 days of treatment with vehicle or MI-3454; n=1 / cohort of mice. MP+BL - Murine progenitors and leukemic blasts, MPr - Myeloid precursors, including neutrophils, EP- Erythroid precursors, EO – Eosinophils, LY – Lymphocytes, MO – Monocytes, BA – Basophils. **E**. Body weight change of NSG mice transplanted with MOLM13 cells during treatment with MI-3454 (100 mg/kg, b.i.d., p.o.) or vehicle (mean ± SD, n = 8). All vehicle-treated mice have died from terminal leukemia by day 11 of treatment. Body weight measurements are reference to the values obtained at the first day of treatment, which were set as 100%. **F**. Pictures of spleen isolated from the vehicle treated mice in the MOLM13 xenograft model at the terminal leukemia stage. **G**. Representative histograms for quantification of hCD45+ cells in the vehicle treated mice in the MOLM13 leukemia model at the terminal leukemia stage. SS – side scatter.

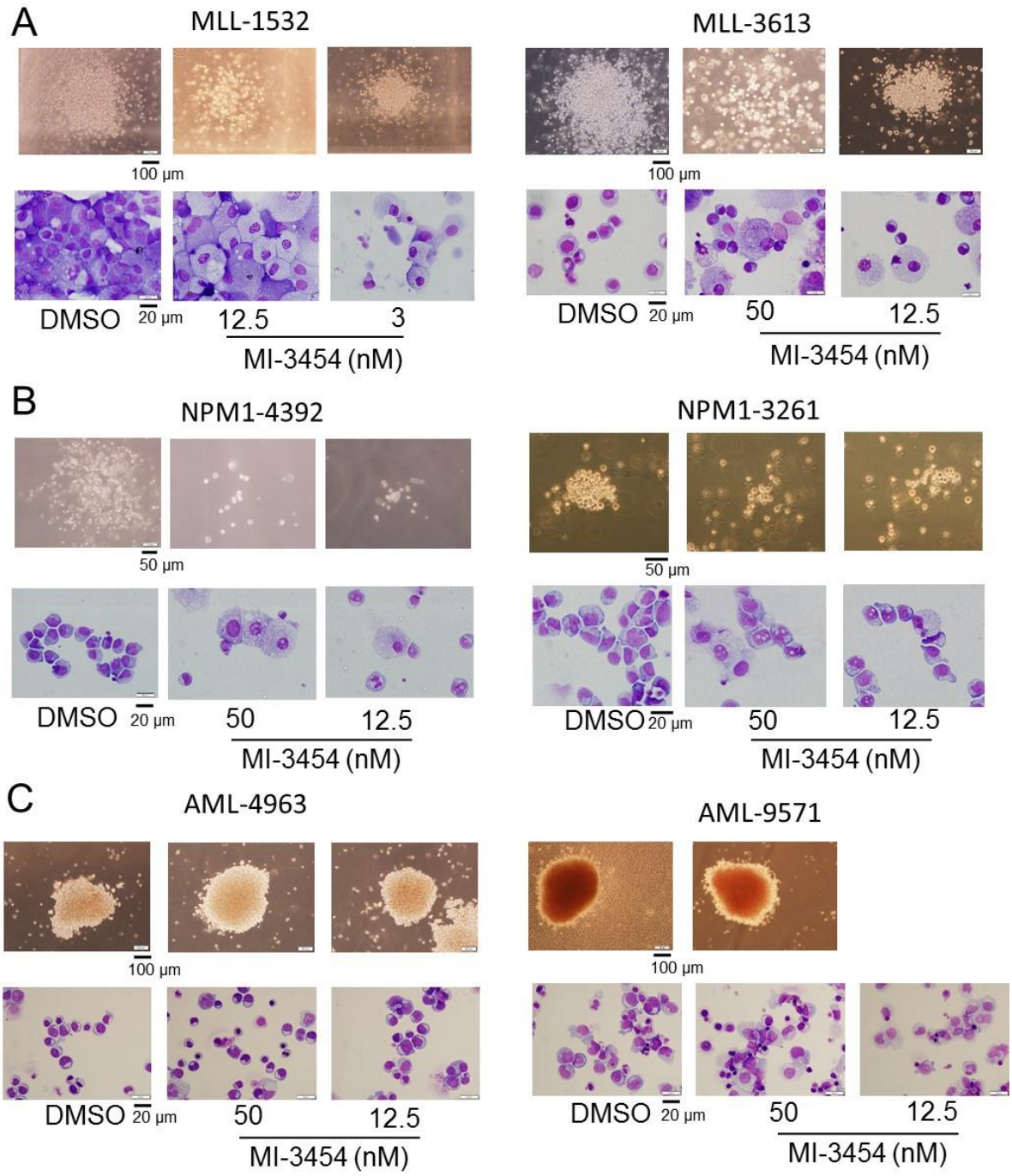

Supplemental Figure 6. Activity of MI-3454 in primary leukemia patient samples. A-C. Pictures of colonies and Wright-Giemsa-stained cytospins for various AML primary patient samples with different mutations upon treatment with MI-3454 or DMSO. Concentrations of MI-3454 as indicated in panels **A-C**. Selected pictures: MLL-1532 (DMSO and 12.5 nM MI-3454 in panel **A**), NPM1-4392 (DMSO and 12.5 nM MI-3454 in panel **B**) and AML-4963 (DMSO and 50 nM MI-3454 in panel **C**) are also presented in **Figure 3E** but are included here as a reference (the DMSO-treated samples) or to demonstrate a dose-dependent effect of MI-3454.

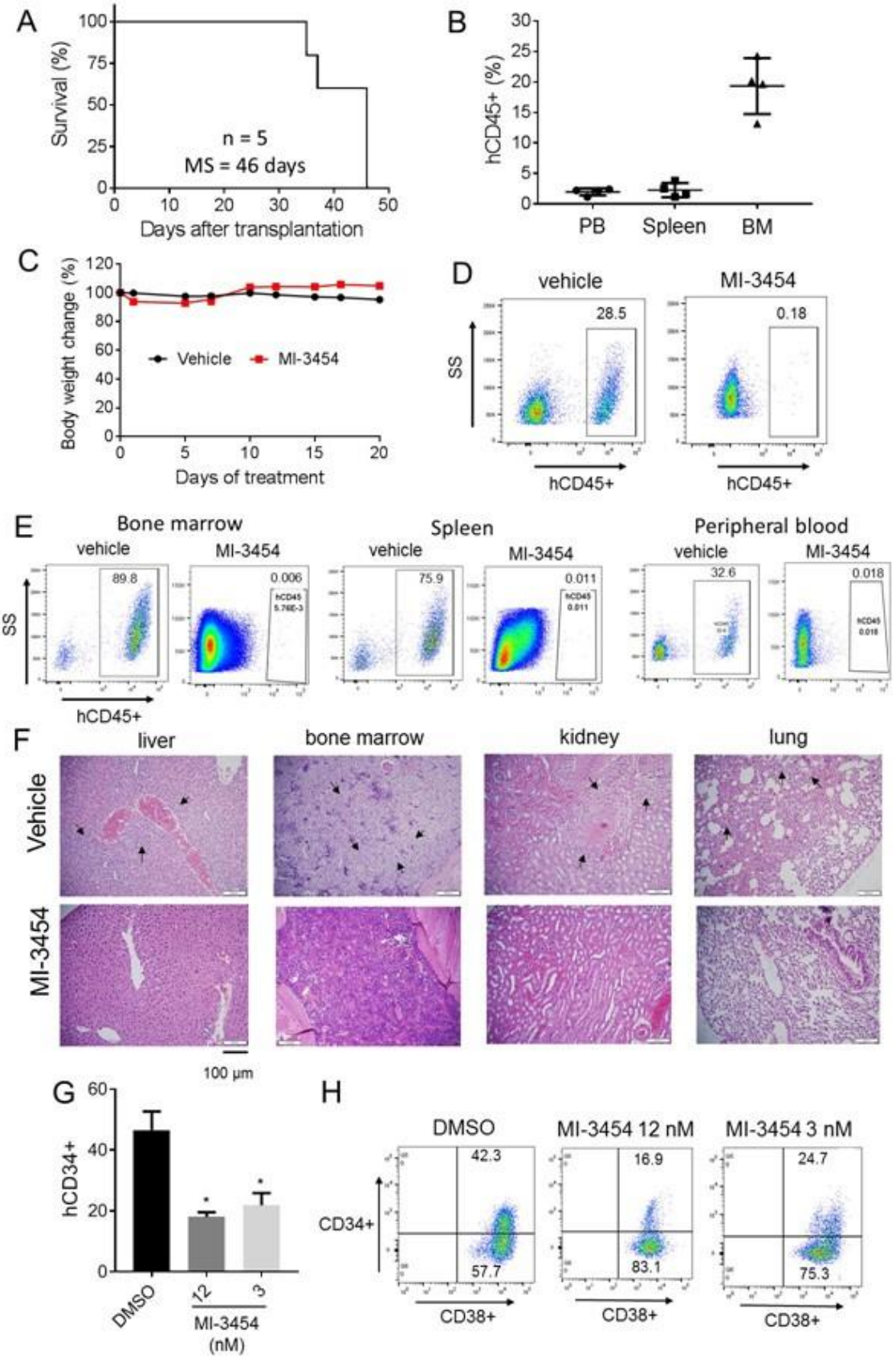
A
Survival (%)
n = 5
MS = 46 days
Days after transplantation
B
hCD45+ (%)
PB
Spleen
BM
C
Body weight change (%)
Vehicle
MI-3454
Days of treatment
D
vehicle
MI-3454
28.5
0.18
SS
hCD45+
E
Bone marrow
Spleen
Peripheral blood
vehicle
MI-3454
89.8
0.006
75.9
0.011
32.6
0.018
SS
hCD45+
F
liver
bone marrow
kidney
lung
Vehicle
MI-3454
100 μm
G
hCD34+
DMSO
12
3
MI-3454 (nM)
H
DMSO
MI-3454 12 nM
MI-3454 3 nM
42.3
57.7
16.9
83.1
24.7
75.3
CD34+
CD38+

Supplemental Figure 7. Activity of MI-3454 in MLL-1532 PDX model. A. Development of MLL-1532 PDX model. Kaplan-Meier survival curve for NSGS mice transplanted with MLL-1532 primary AML sample. MS – median survival. **B**. Level of hCD45+ cells in MLL-1532 PDX model measured by flow cytometry in bone marrow (BM), spleen and peripheral blood (PB) before initiating treatment with MI-3454. Mean ± SD, n = 4. **C**. Body weight change of NSGS mice in the MLL-1532 PDX during treatment with MI-3454 (100 mg/kg, b.i.d., p.o.) or vehicle (mean ± SD, n = 8). Body weight measurements are reference to the values obtained at the first day of treatment, which were set as 100%. **D.** Representative histograms for quantification of hCD45+ cells by flow cytometry in blood samples isolated from MLL-1532 PDX model after 19 days of treatment with vehicle or MI-3454. **E**. Representative histograms for quantification of hCD45+ cells by flow cytometry in bone marrow, spleen and blood samples isolated from MLL-1532 PDX model after treatment with vehicle (samples collected at the terminal leukemia stage, days 33-51 post-transplantation) or MI-3454 (samples collected at day 164 post-transplantation). SS – side scatter. **F**. Histological sections of liver parenchyma, bone marrow (sternum), kidney and lung samples from vehicle (upper panel) or MI-3454 (100 mg/kg, b.i.d., p.o.) treated MLL-1532 mice. Black arrows indicate regions of infiltration with leukemic blasts. Photographs of sections were taken using 10x and 100x objectives with Olympus BX-51 microscope. **G. H.** MI-3454 reduces the level of human CD34+ cells in MLL-1532 primary AML sample. hCD34+ cells were sorted out from the bulk of leukemia cells and cultured on MS-5 stromal cells for three week, during which MI-3454 or DMSO were used for treatment. Quantification of human CD34+ cells (**G**) and representative histograms demonstrating the level of CD34 progenitor markers (**H**) are shown. Mean ± SD, n = 2. All CD34+ cells were positive for the presence of CD38 progenitor marker. The anti-CD34 (BioLegend, cat. #343514, clone: 581) and anti-CD38 (Invitrogen, cat. #12-0388-42, clone: HB7) antibodies were used for detection of progenitor cells.

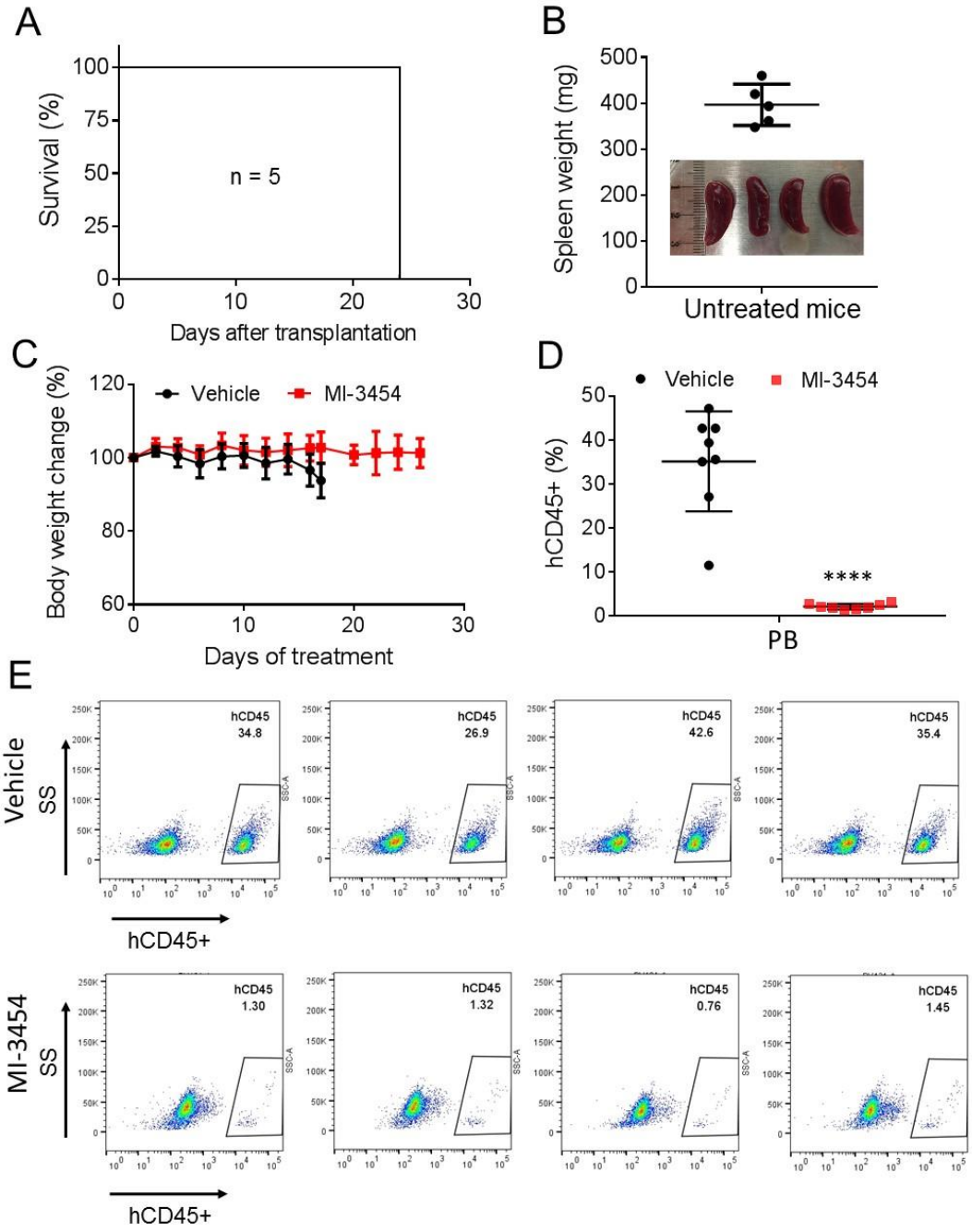

Supplemental Figure 8. Activity of MI-3454 in MLL-449 PDX model of infant ALL. A. Development of MLL-449 PDX model of infant ALL. Survival of mice is shown for untreated mice. **B**. Spleen size for mice at the stage of terminal leukemia in the MLL-449 PDX mouse model. Mean ± SD, n = 5. **C**. Body weight change in NSGS mice in the MLL-449 infant ALL PDX model during treatment with MI-3454 (100 mg/kg, b.i.d., p.o.) or vehicle (mean ± SD, n = 8). Body weight measurements are reference to the values obtained at the first day of treatment, which were set as 100%. All vehicle-treated mice died by d17 of treatment due to terminal leukemia. **D, E.** Quantification (**D**) and representative histograms (**E**) from flow cytometry analysis of peripheral blood samples of the MLL-449 PDX mice after treatment with vehicle or MI-3454 performed at day 17 of treatment. mean ± SD, n = 8, **** $p < 0.0001$ calculated using Student's 2-tailed t-test. SS – side scatter.

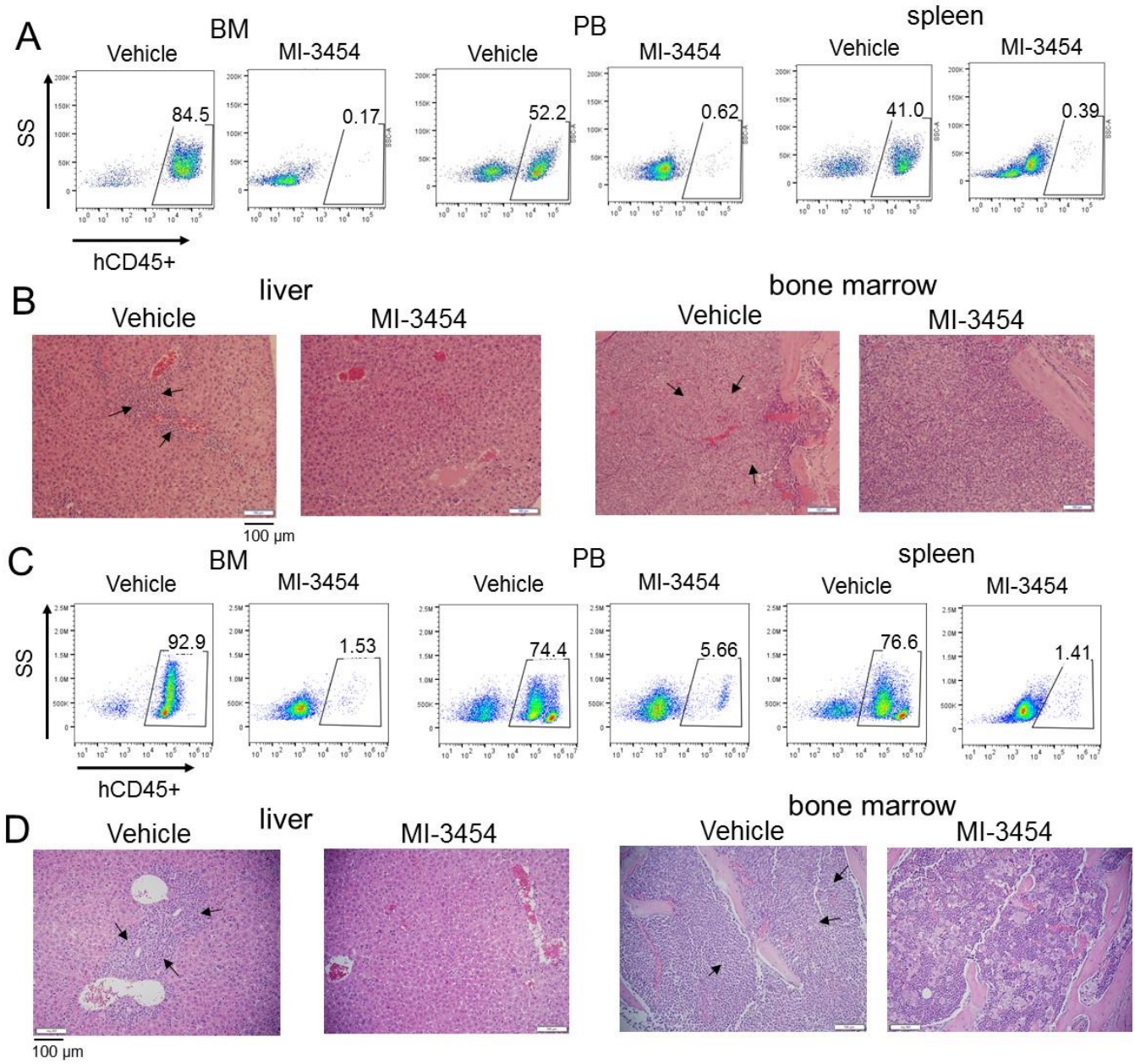

Supplemental Figure 9. ***In vivo*** **activity of MI-3454 in the PDX models of** ***NPM1*****-mutated AMLs. A** and **C.** Representative histograms from quantification of hCD45+ cells in bone marrow (BM), peripheral blood (PB) and spleen of mice in the NPM1-3055 (**A**) or NPM1-4392 (**C**) PDX models upon treatment of mice with MI-3454 (100 mg/kg, b.i.d., p.o.) or vehicle. Samples were collected at the end point of the experiments. SS – side scatter. **B** and **D**. Histological sections of organs from vehicle- or MI-3454-treated (100 mg/kg, b.i.d., p.o.) NPM1-3055 (**B**) and NPM1-4392 (**D**) PDX mice. Black arrows indicate regions of infiltration with leukemic blasts. Photographs of sections were taken using 10x and 100x objectives with Olympus BX-51 microscope.

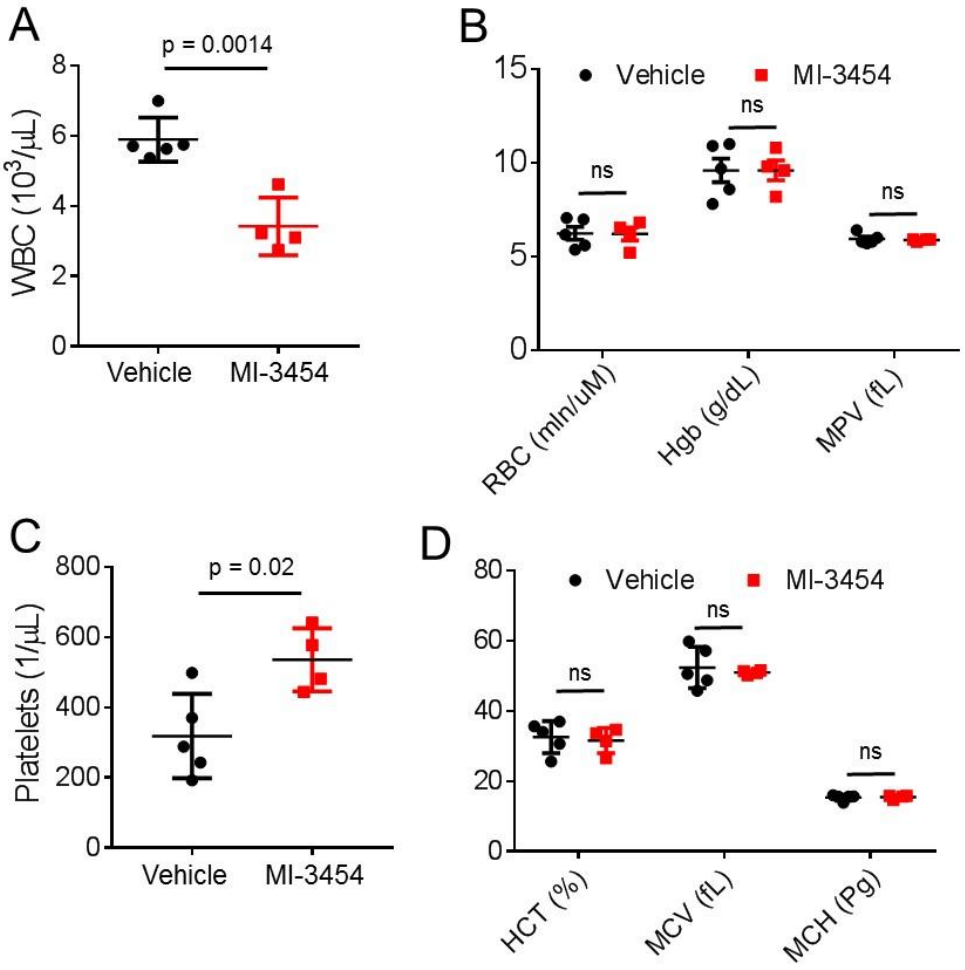

Supplemental Figure 10. Analysis of blood counts in PDX model with *NPM1* mutation upon treatment with MI-3454. A-D. Analysis of blood cell counts (WBC – white blood cells, RBC – red blood cells, Platelets) and other blood parameters (Hgb – Hemoglobin, MPV – Mean Platelet Volume, HCT-Hematocrit, MCV – Mean corpuscular volume, MCH - Mean corpuscular hemoglobin) in the NPM1-3055 PDX mice after treatment with vehicle or MI-3454 (100 mg/kg, b.i.d., p.o.). Samples were collected at the end point of the experiment. Mean +/- SD, n = 5, ns – not significant. Statistical significance was calculated using Student's 2-tailed t-test.

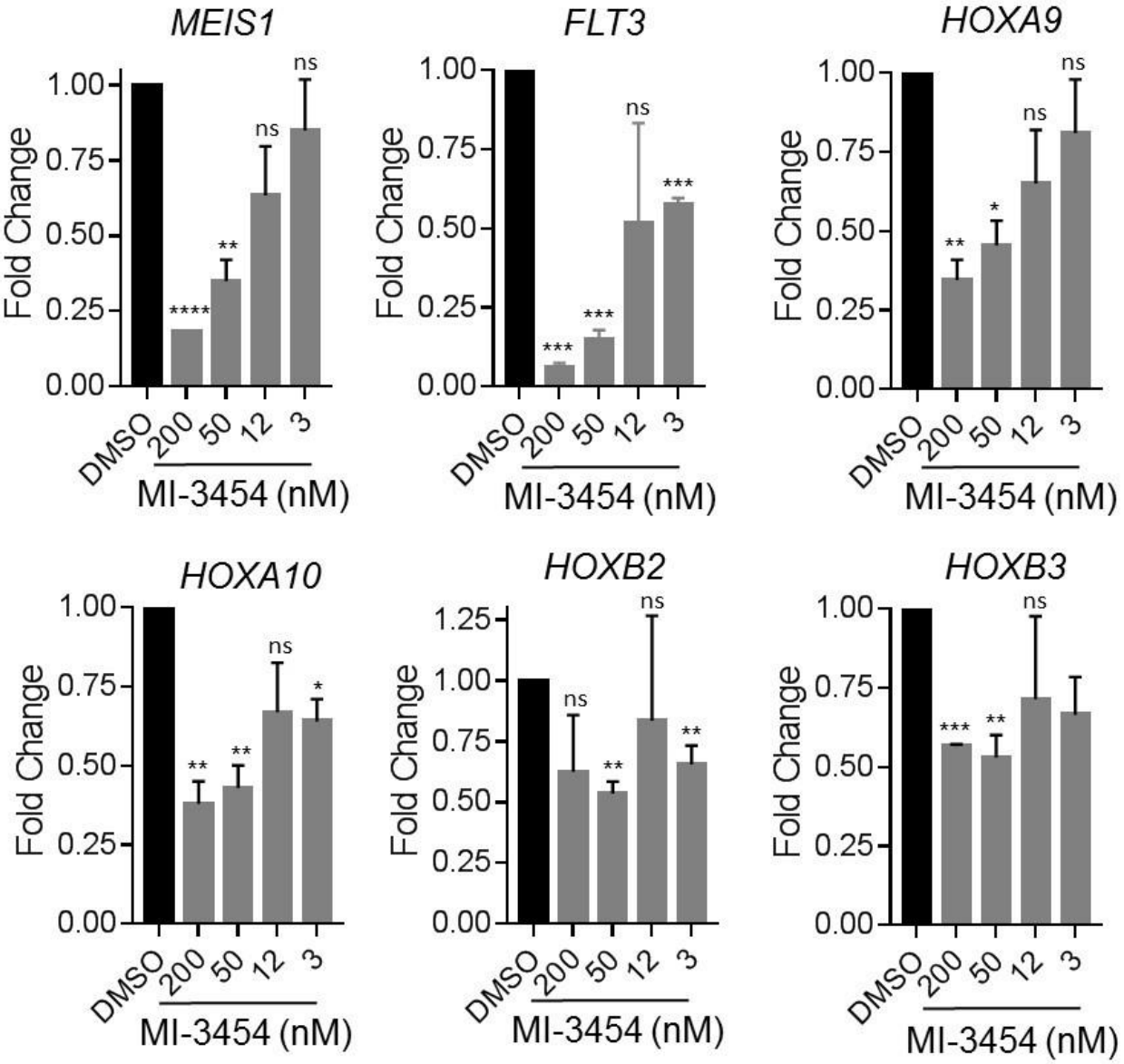

Supplemental Figure 11. Gene expression studies in the *NPM1*-mutated #5046 primary sample. Mean ± SD, n = 2. *p<0.05, **p<0.01, ***p<0.001, ****p<0.0001, ns – not significant, calculated using Student's 2-tailed t-test.

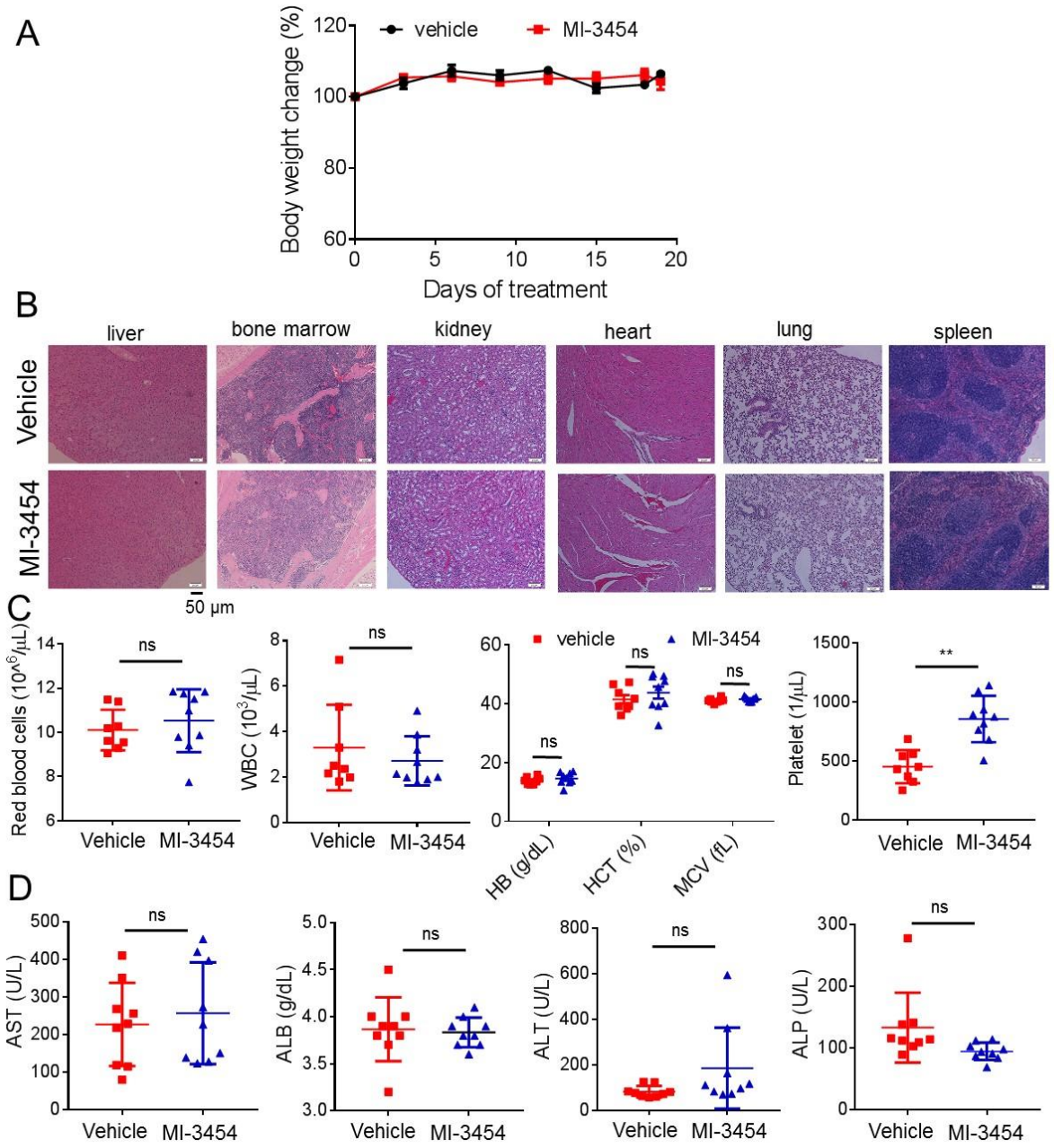

Supplemental Figure 12. Effect of MI-3454 in normal mice. A. Body weight change in normal C57BL/6 mice after 19 days of treatment with MI-3454 (100 mg/kg, b.i.d., p.o.) or vehicle (mean ± SD, n = 9). Body weight measurements are reference to the values obtained at the first day of treatment, which were set as 100%. **B**. Histopathology of organs in normal C57BL/6 mice after 19 days of treatment with MI-3454 or vehicle. **C**. Analysis of blood cell counts (WBC – white blood cells, RBC – red blood cells, Platelets) and other blood parameters (Hgb – Hemoglobin, HCT- Hematocrit, MCV – Mean corpuscular volume) in normal mice after treatment with vehicle or MI-3454. **D**. Analysis of liver panel enzymes in blood samples isolated from normal mice upon treatment with MI-3454 or vehicle. In panels **C** and **D**, samples were collected at the end point of the experiment after 19 days of treatment. Mean +/- SD, n = 9, ns – not significant, **p<0.01 calculated using Student's 2-tailed t-test.

.

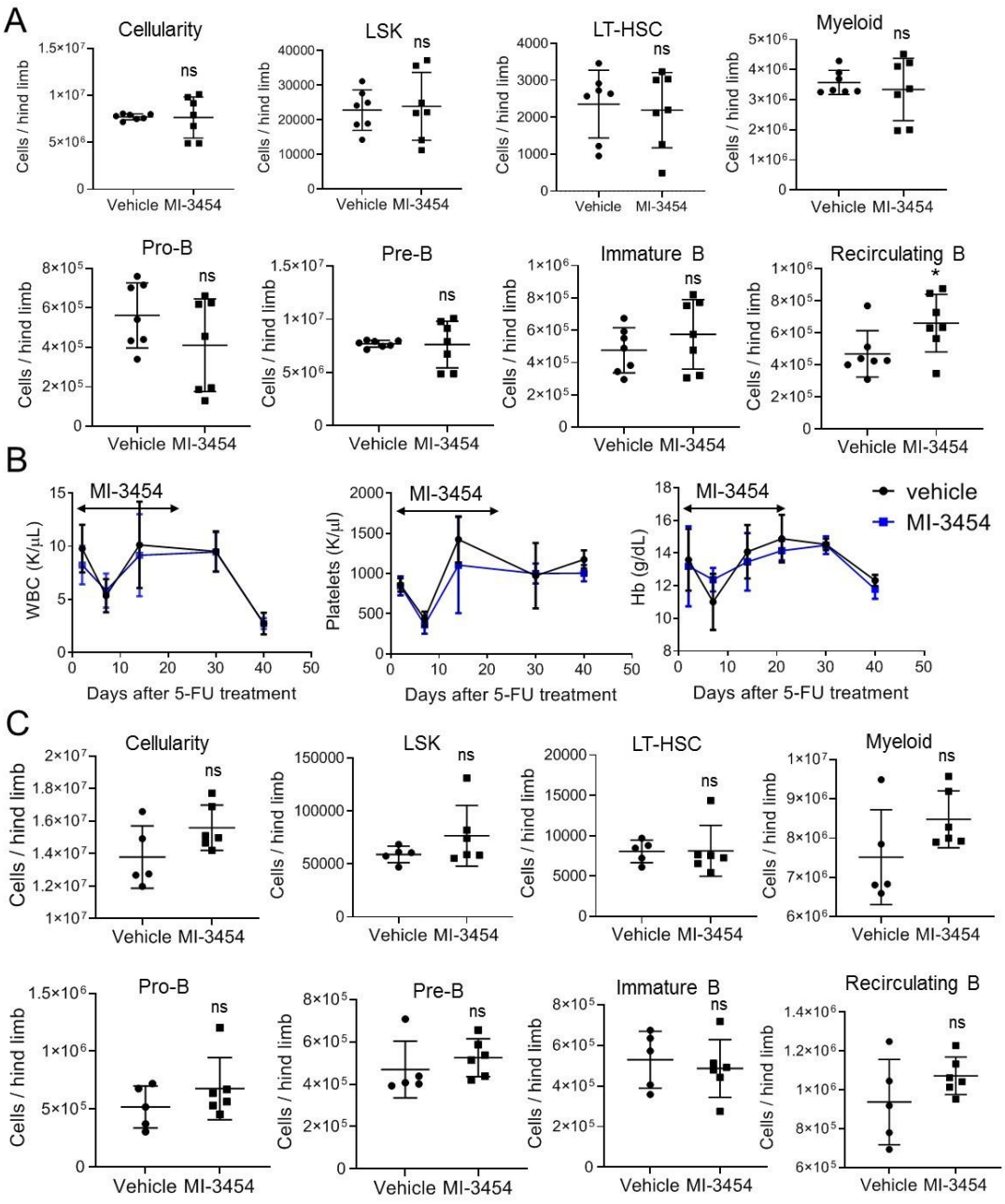

Supplemental Figure 13. Effect of MI-3454 on hematopoietic reconstitution after transplant and on hematopoietic recovery after 5-FU treatment. A. Analysis of bone marrow samples from C57BL/6 CD45.2 recipient mice transplanted with bone marrow isolated from B6 CD45.1 donor mice after 21 days treatment with MI-3454 (100 mg/kg, b.i.d., p.o.) or vehicle (n = 7, mean ± SD) followed by additional 20 days of mice monitoring. *p<0.05, ns – not significant, calculated using Student's 2-tailed t-test. **B.** Analysis of blood cell counts (WBC, Platelets) and hemoglobin level (Hb) in C57BL/6 mice treated with 5-FU followed by 21 days administration of MI-3454 (100 mg/kg, b.i.d., p.o.) or vehicle. Mean ± SD, n = 6. Difference is not significant between vehicle and MI-3454 cohorts for any of the blood parameters shown as calculated using 2-way ANOVA with Sidak multiple comparison test **C.** Analysis of bone marrow samples from C57BL/6 mice after 5-FU treatment followed by administration of MI-3454 or vehicle and additional 20 days of mice monitoring. ns – not significant as calculated using Student's 2-tailed t-test. Treatment regimen as in **B**.

Data collection	
Space group	$P2_12_12_1$
Cell dimensions	
a, *b*, *c* (Å)	49.09, 79.84, 124.26
α, β, γ (°)	90.0, 90.0, 90.0
Resolution (Å)	50-1.24 (1.28-1.24)
R_{sym} or R_{merge}	0.079 (0.697)
$I / \sigma I$	18.03 (2.63)
Completeness (%)	99.8 (98.6)
Redundancy	7.2 (6.8)
Refinement	
Resolution (Å)	27.72-1.24
No. reflections	138,482
R_{work} / R_{free}	16.26 / 18.69
No. atoms	
Protein	3737
Ligand/ion	85
Water	859
B-factors (Å^2)	
Protein	17.49
Ligand/ion	29.19
Water	36.14
R.m.s. deviations	
Bond lengths (Å)	0.008
Bond angles (°)	0.99

Supplemental Table 1. Data collection and refinement statistics for menin-MI-3454 complex. All diffraction data were obtained from a single crystal. Values in parentheses are for highest-resolution shell.

Sample ID	Disease	Chromosomal abnormality	Mutations / Chromosomal abnormality
MLL-1532	AML	11q23	MLL-p300
MLL-3613	AML	11q23	MLL-AF9
MLL-181	AML	11q23	MLL-ENL
MLL-1236	AML	11q23	MLL-AF9
NPM1-3261	AML	Normal cytogenetics	NPM1, FLT3-ITD
NPM1-3055	AML	Normal cytogenetics	NPM1, FLT3-ITD
NPM1-4392	AML	Normal cytogenetics	NPM1, DNMT3A, TET2
NPM1-4144	AML	Normal cytogenetics	NPM1, IDH2
NPM1-4607	AML	Normal cytogenetics	NPM1, TET2
NPM1-5046	AML	Normal cytogenetics	NPM1, DNMT3A, TET2, FLT3-ITD
AML-4963	AML	Normal cytogenetics	FLT3, U2AF1, ZRSR2, WT1
AML-9571	AML	Normal cytogenetics	FLT3-ITD, IDH
AML-5696	AML	Normal cytogenetics	FLT3, WT1, ASX1

Supplemental Table 2. Characterization of primary patient samples used for testing MI-3454 menin-MLL1 inhibitor.

SUPPLEMENTAL MATERIALS AND METHODS

Biochemical characterization of MI-3454 menin-MLL inhibitor

Inhibition of the menin-MLL1 interaction by MI-3454 was assessed by fluorescence polarization (FP) assay using the protocol described previously (3). In the competition FP experiment, menin was used at 4 nM, fluorescein labeled $MLL1_{4-43}$ peptide (FLSN_$MLL1_{4-43}$) was used at 4 nM and a broad range of concentrations of MI-3454 was applied.

Crystallographic data collection and structure determination

Diffraction data for menin-MI-3454 complex were collected at the 21-ID-D beamline at the Life Sciences Collaborative Access Team at the Advanced Photon Source. Data were processed with HKL-2000 (4). Structure of the complex was determined by molecular replacement using MOLREP with the apo-structure of human menin (PDB code: 4GPQ) as a search model in molecular replacement. The model was refined using REFMAC (5), COOT (6), CCP4 (7) and PHENIX (8) packages. Final structure was refined using anisotropic refinement. Validation of the structure was performed using MOLPROBITY (9) and ADIT (10). Details of data processing and refinement are summarized in **Table S1**.

Liver microsomal stability

The *in vitro* metabolic stability of MI-3454 (0.5 µM) was evaluated with pooled male liver microsomes (0.3 mg/mL), which were incubated at 37°C in the presence of an NADPH-generating system containing 100 mM, pH 7.4 potassium phosphate buffer, 3.3 mM magnesium chloride, 1 mM EDTA, 1.3 mM NADP, 3.3 mM glucose-6-phosphate, and 0.6 Unit/mL of glucose-6-phosphate dehydrogenase. After protein precipitation by acetonitrile, the level of remaining MI-3454 was analyzed by LC/MS/MS.

Inhibition of human P450 enzymes

Inhibition of seven major CYP enzymes by MI-3454 (10 µM) was evaluated using standard substrates (Dextromethorphan for CYP2D6; Diclofenac for CYP2C9; Midazolam for CYP3A4; S-mephenytoin for CYP2C19; Tacrine for CYP1A2; Amodiaquine and CYP2C8) in male human liver microsomes (0.2 mg/mL), which were incubated in the NADPH-generating system (described in the liver microsomal stability method section) at 37°C for 12 minutes. The metabolism of each substrate in human liver microsomes was associated with a specific CYP-mediated metabolite, which was monitored by LC/MS/MS to reflect activity of individual CYP isoforms.

Kinetics solubility

Kinetics solubility of MI-3454 (100 µM) was evaluated in PBS buffer (pH 7.4, 1% DMSO) by overnight incubation at room temperature. After centrifugation for 10 min at 22 °C, the concentration of MI-3454 in the supernatant was analyzed by the LC/MS/MS system. Solubility of MI-3454 in DMSO was also evaluated in the same incubation conditions and used as a reference.

Real-Time PCR

The following Taqman probes were used to quantify expression of individual genes: *GAPDH*: Hs99999905_m1, *HPRT1*: Hs02800695_m1, *HOXA9* Hs00365956_m1, *HOXA10*: Hs00172012_m1, *HOXB2*: Hs01911167_m1, *HOXB3*: Hs00231127_m1, *HOXB4*: HS00256884_m1, *DLX2*: Hs00269993_m1, *FLT3*: Hs00174690_m1, *MEF2C*: Hs00231149_m1, *MEIS1*: Hs00180020_m1, *MNDA*: Hs00935905_m1, *PBX3*: Hs00608415_m1.

Colony assays

Patient samples were thawed and cultured in IMDM medium with 20% BIT9500 (STEMCELL), 1% penicillin/streptomycin, 16.7 µg/mL human LDL (STEMCELL,), 55 µM β-mercaptoethanol, 20 ng/mL IL6, 20 ng/mL IL3, 20 ng/mL GCSF, 20 ng/mL GM-CSF, 50 ng/mL FLT, 50 ng/mL SCF for 4-24 hours. The cells were then mixed with DMSO or MI-3454 in MethoCult Express (STEMCELL), plated at 10,000-50,000 cells/mL on 35 mm culture dish and cultured for 7 to 10 days to form colonies.

Animal use

All animal experiments in this study were approved by the University of Michigan Committee on Use and Care of Animals and Unit for Laboratory Animal Medicine (ULAM).

PK studies in mice

The pharmacokinetics of MI-3454 menin-MLL inhibitor was determined in female CD-1 mice (Charles River) following intravenous (i.v.) dosing at 15 mg/kg and oral dosing (p.o.) at 100 mg/kg. MI-3454 was dissolved in the vehicle containing 20% (v/v) (2-Hydroxypropyl)-β-cyclodextrin and 5% (v/v) Cremophore. Serial blood samples (70 µL) were collected over 24 h, centrifuged at 15,000 rpm for 10 min to get plasma for analysis. For PK studies in brain and cerebrospinal fluid (CSF), plasma, brain and CSF samples were collected from mice at 3, 7 and 24 h after dosing with MI-3454 (100 mg/kg, p.o.). Plasma, brain and CSF concentrations of MI-3454 was determined by the LC-MS/MS method developed and validated for this study. The LC-MS/MS method consisted of a Shimadzu UFLC 20A system and chromatographic separation

of test compound was achieved using an Agilent Zorbax Extend-C18 column (5 cm x 2.1 mm, 3.5 µm). An AB Sciex QTrap 4500 mass spectrometer equipped with an electrospray ionization source (ABI-Sciex, Toronto, Canada) in the positive-ion multiple reaction monitoring (MRM) mode was used for detection. All pharmacokinetic parameters were calculated by noncompartmental methods using WinNonlin® version 3.2 (Pharsight Corporation, Mountain View, CA, USA). Parameters are presented as a mean ± standard deviation (SD).

Mouse histology and tissue sample preparation

Tissues were fixed with 10% neutral buffered formalin and submitted for sectioning to the Pathology Cores for Animal Research at the University of Michigan. Photographs of sections were taken using 10x and 100x objectives with Olympus BX-51 microscope. Peripheral blood samples were collected in EDTA-treated tubes and sent for complete blood counts to ULAM laboratory at the University of Michigan. Peripheral blood samples were also collected in non-treated tubes and sent for liver panel tests to ULAM laboratory. Bone marrow cells were isolated by flushing both femurs and tibias with DMEM with 5% FBS. Single cell cytospins were stained with the HEMA3 stain Kit (Thermo Fisher Scientific).

Analysis of stress hematopoiesis in vivo

For analysis of the effect of MI-3454 on 5-fluorouracil (5-FU) induced stress hematopoiesis in vivo, 8-10 weeks old female C57BL/6 mice (Taconic Farms) were treated with a single dose of 150 mg/kg of 5-FU in PBS via i.p. administration. The following day treatment with vehicle or MI-3454 (100 mg/kg, p.o., b.i.d.) was initiated and continued for 21 days. Blood samples were collected once per week for analysis of complete blood counts and to assess populations of myeloid (CD11b+/Gr-1+), B- (B220+/CD19+) and T- (CD3+) cells. The following antibodies from BioLegend were used for staining: anti-CD11b (#101208, MI/70), Gr-1 (#108433, RB6-8C5), B220 (#103224, RA3-6B2), CD19 (#115520, 6D5), CD3 (#109211, H57-597). At the end point of the experiment (three weeks after completing the treatment with MI-3454), bone marrow and blood samples were collected, processed and analyzed in the same manner as in normal mice without 5-FU treatment (see above). For testing the effect of MI-3454 on hematopoietic reconstitution after transplantation, 8-10 week old female C57BL/6 (CD45.2) recipient mice (Taconic Farms) were lethally irradiated with 9.0 Gy. Six hours later, 1 mln of bone marrow cells isolated from 8-10 weeks old female B6.SJL (CD45.1) donor mice (Jackson Laboratory) were transplanted to the recipient mice via tail vein injection. Treatment of the recipient mice with vehicle or MI-3454 was initiated on the second day after transplantation and was continued for 21 days. Blood samples were collected once per week for analysis of complete blood counts, the percentage of CD45.1+donor-derived cells among B-, T-, and

myeloid cell populations. At the end point of the experiment (three weeks after completing the treatment), bone marrow and blood samples were isolated and analyzed in a similar way as in the 5-FU treated mice. Antibodies to detect donor and recipient cells, CD45.1 (#110724, A20) and CD45.2 (#109836, 104) were purchased from BioLegend.

Chemical synthesis of MI-3454

General Information

All commercially available solvents and reagents were used without further preparation unless otherwise indicated. The ^{1}H and ^{13}C NMR data were taken on Bruker Advance III 600 MHz or Varian MR400 (fluorine spectra). Chemical shifts are reported in ppm relative to tetramethylsilane or residual solvent signal. Some signals that overlapped with solvents were identified using ^{1}H-^{13}C HSQC spectrum (multiplicity not known). The mass measurements were determined on Agilent Q-TOF time-of-flight mass spectrometer using positive ion mode and electrospray ionization. Analytical TLC was performed on Merck TLC aluminum plates precoated with F_{254} silica gel 60 (UV, 254 nm, and iodine). The purity analysis of final compounds was determined on Shimadzu Prominence HPLC system (20 series: binary pump, UV/Vis at 254 nm, heated column compartment 28 °C), using Restek Ultra C18 (5 μm) 150 mm × 4.6 mm column. LC-MS spectra were recorder on Shimadzu LC-2020 system (DUIS-ESI). The solvents were programmed to run at gradient starting at 10 % CH_3CN in water from 1 min to 80% during 8 min run. If not indicated, the purity of all final compounds was >95% as determined by HPLC via integration of UV spectra at 254 nm. Main intermediates were purchased from Enamine (compound **2,** EN300-1590404) and from PharmaBlock (3-((*tert*-butoxycarbonyl)amino)bicyclo[1.1.1]pentane-1-carboxylate).

Abbreviations

AcCN	Acetonitrile
Ac	Acetyl
DIPEA	*N*,*N*-Diisopropylethylamine
DMAP	4-Dimethylaminopyridine
DCM	Dichloromethane
DMF	Dimethylformamide
DMSO	Dimethyl Sulfoxide
Et	Ethyl
ESI	Electrospray Ionization
HR-MS	High Resolution Mass Spectrometry

iPr	*Iso*-propyl
MsCl	Methanesulfonyl chloride
TEA	Triethylamine
TFA	Trifluoroacetic acid
THF	Tetrahydrofuran
rt	room temperature

Scheme 1. Synthetic scheme for preparation of MI-3454

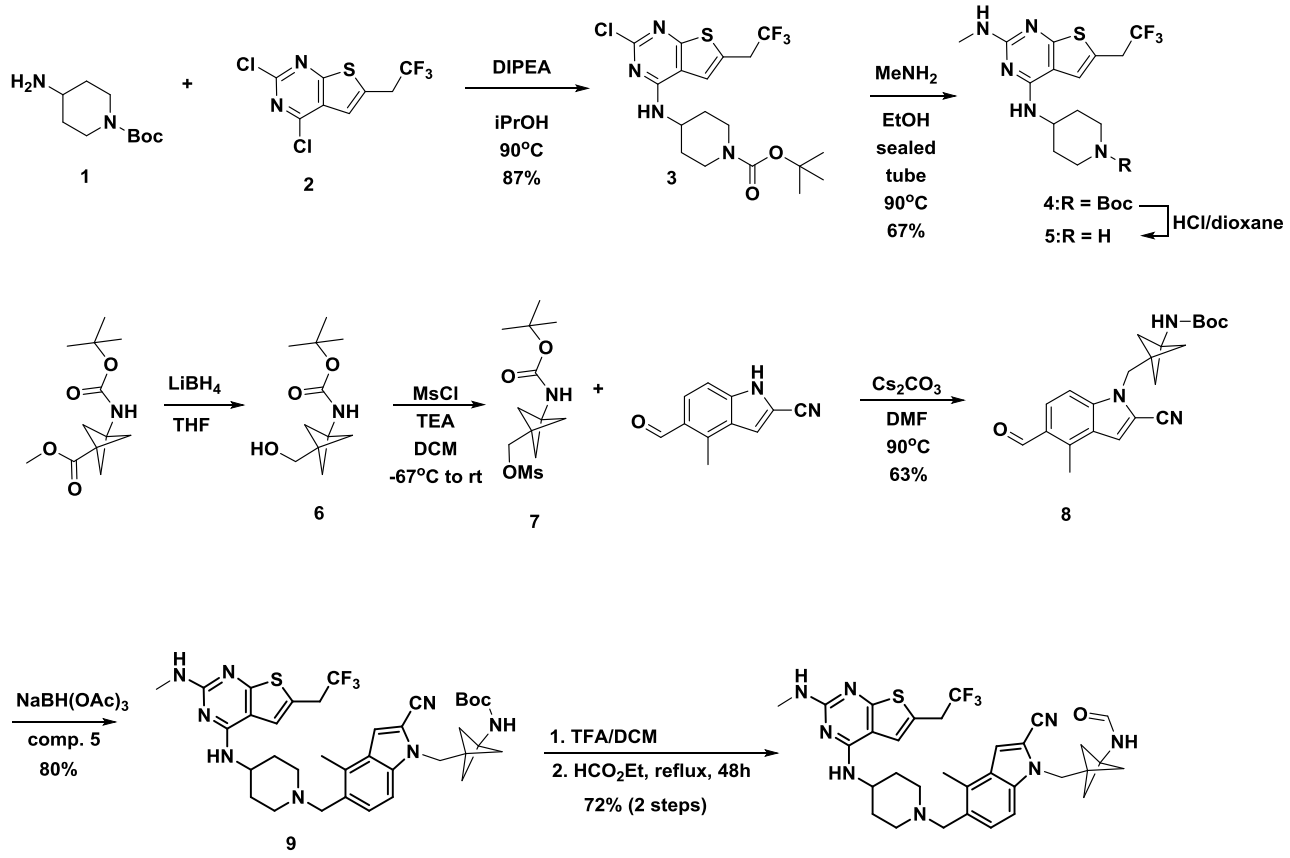

Synthesis of MI-3454

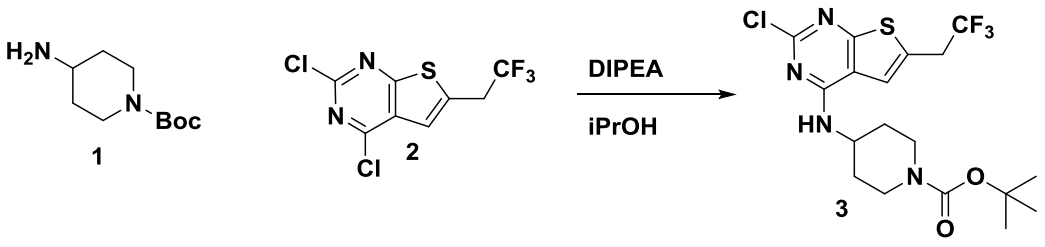

***tert*-butyl 4-((2-chloro-6-(2,2,2-trifluoroethyl)thieno[2,3-d]pyrimidin-4-yl)amino)piperidine-1-carboxylate (3)** 2,4-dichloro-6-(2,2,2-trifluoroethyl)thieno[2,3-d]pyrimidine (**2**, 3g, 10.5 mmol) was suspended in 2-propanol (15 mL) and DIPEA (3.6 mL, 2.0 eq, 21 mmol) was added. Then *tert*-butyl 4-aminopiperidine-1-carboxylate (**1**, 2.3 g, 1.1 eq, 11.6 mmol) was added and mixture was stirred at 90 °C overnight. Precipitate was formed when cooled. The reaction mixture was diluted with MeOH, mixed with silica gel and thoroughly dried. The reaction crude was purified using flash chromatography (80g prepacked silica gel column, hexane-ethyl acetate, 0% - 50% EtOAc, 15 min. Washed at 50% EtOAc. Compound **3** was isolated as pale yellow solid (4.1g, 87% yield). HR-MS [M+H$^+$]: m/z calculated: 451.1182, found: 451.1183.

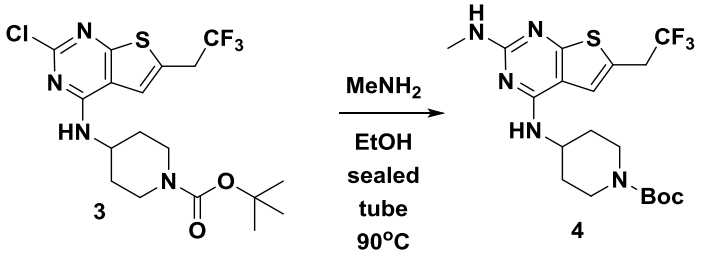

***tert*-butyl 4-((2-(methylamino)-6-(2,2,2-trifluoroethyl)thieno[2,3-d]pyrimidin-4-yl)amino)piperidine-1-carboxylate (4).** Compound **3** (4.04 g, 9 mmol) was suspended in ethanol (22 mL) and mixed with 33% solution of methylamine in absolute ethanol (5.6 mL, 5 eq, 45 mmol). TEA (6.2 mL, 5 eq, 45 mmol) was added and the tube was sealed tightly. The mixture was heated at 90 °C overnight. The reaction mixture was transferred to a round bottom flask and diluted with MeOH. Silica gel was added and solvent was thoroughly evaporated. The reaction crude was then purified using flash chromatography (silica gel prepacked 80g column, hexane-ethyl acetate) to afford 2.7 g (67% yield) of compound **4**. ^{1}H NMR (600 MHz, DMSO-d$_6$) δ 7.34 (s, 1H), 7.18 - 7.31 (m, 1H), 6.43 - 6.63 (m, 1H), 4.14 - 4.25 (m, 1H), 3.88 - 4.00 (m, 2H), 3.82 (q, *J* = 10.9 Hz, 2H), 2.81 - 2.98 (m, 2H), 2.77 (d, *J* = 4.0 Hz, 3H), 1.85 - 1.95 (m, 2H), 1.36 - 1.51 (m, 2H), 1.41 (s, 9H); ^{13}C NMR (151 MHz, DMSO-d6) δ 168.9, 160.4, 156.0, 153.9, 125.7 (*J* = 277.3 Hz), 121.2, 118.5, 108.8, 78.6, 54.8, 46.8, 33.9 (*J* = 30.8Hz), 31.3, 28.0, 27.9 LC-MS M/Z [M+H$^+$] m/z: 446.1

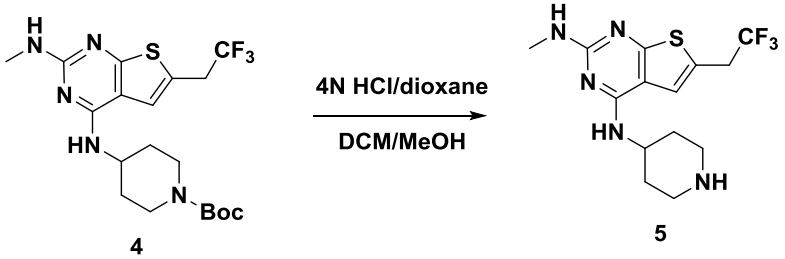

N^2-methyl-N^4-(piperidin-4-yl)-6-(2,2,2-trifluoroethyl)thieno[2,3-d]pyrimidine-2,4-diamine (5). Compound **4** (2.7g, 6 mmol) was dissolved in a mixture of DCM and MeOH (29 mL, 10:1, *v/v*) before 6.8 mL of 4N HCl in dioxane was added. Precipitate was formed after 2 hours and LC-MS indicated no starting material remained. The reaction mixture was diluted with DCM/MeOH (10:1, v/v, 150 mL) and washed with conc. aqueous ammonia solution. The organic phase was separated and the aqueous phase was basified with 1M NaOH until pH=14. The aqueous phase was extracted with 100 mL of DCM. Combined organic phases were washed with brine and dried over sodium sulfate. The organic solution was filtered and dried to afford a yellowish oil. DCM was added and evaporated repeatedly until a pale yellow solid was formed. ^{1}H NMR (600 MHz, methanol-d4) δ 7.23 (s, 1H), 4.14 - 4.26 (m, 1H), 3.64 (q, J = 10.5 Hz, 2H), 3.06-3.14 (m, 2H), 2.91 (s, 3H), 2.62 - 2.75 (m, 2H), 1.99 - 2.11 (m, 2H), 1.46 - 1.58 (m, 2H); ^{13}C NMR (151 MHz, chloroform-d) δ 169.9, 162.4, 158.2, 126.6 (*J* = 276.2 Hz), 121.9, 121.7 (*J* = 3.3Hz), 111.1, 49.1, 46.4, 35.8 (*J* = 30.8Hz), 33.7, 28.7; HR-MS [M+H$^+$]: m/z calculated: 346.1308, found: 346.1309

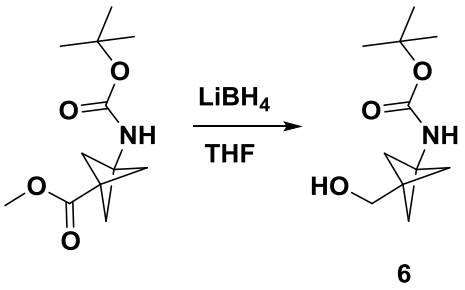

***tert*-butyl (3-(hydroxymethyl)bicyclo[1.1.1]pentan-1-yl)carbamate (6).** methyl 3-((*tert*-butoxycarbonyl)amino)bicyclo[1.1.1]pentane-1-carboxylate (3g, 12.5 mmol) was suspended in dry THF (59.2 mL) and lithium borohydride (547 mg, 24.9 mmol) was added at 0 °C. Ice batch was removed and the reaction mixture was stirred overnight. 150 mL of EtOAc was added, followed by 5 mL of methanol, 25 mL of water and 20 mL of saturated ammonium chloride solution. The aqueous phase was extracted with 100 ml of EtOAc. Combined organic phases were washed with brine and dried over magnesium sulfate. Organic solvents were removed to provide compound **6** as a white solid. ^{1}H NMR (600 MHz, chloroform-d) δ 4.94 (br. s., 1H), 3.70 (s, 2H), 1.94 (s, 6H), 1.60 (s, 1H), 1.45 (s, 9H).

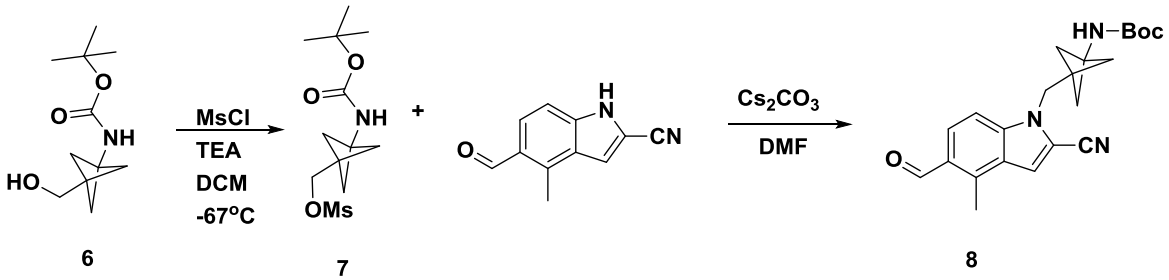

***tert*-butyl (3-((2-cyano-5-formyl-4-methyl-1H-indol-1-yl)methyl)bicyclo[1.1.1]pentan-1-yl)carbamate (8).** TEA (2 ml, 1.8 eq, 14.4 mmol) was added to a suspension of compound **6** (1.7 g, 8 mmol) in 40 mL of DCM to result in a clear solution. The mixture was cooled to -67 ^{o}C and MsCl (938 µL, 1.5 eq, 12.1 mnmol) in DCM (1 mL) was added over a period of 30 min. The reaction mixture became slurry, and additional 10 mL of DCM was added. After stirring for 15 min in dry ice/acetone bath, the reaction was allowed to warm to rt and was it was further stirred for additional 2h. 100 mL of DCM was then added and organic solution was washed with 10% citric acid (2x30 mL), saturated sodium carbonate (2x30 mL) and 30 mL of brine. After removal of volatiles, crude mesylate (**7**) was used in the next step directly. 5-formyl-4-methyl-1H-indole-2-carbonitrile (892 mg, 5.0 mmol, synthesized as described previously (1) and cesium carbonate (4.7 g, 14.5 mmol, 3 eq) were suspended in DMF (14 mL). Crude mesylate (**7,** 8 mmol, 1.6 eq) was added and the reaction was carried out at 90 ^{o}C until no starting aldehyde was present in the mixture. Water was then added followed by ethyl acetate (2 x 100 mL). Combined organic phases were washed with brine 3 times and dried over sodium sulfate. The reaction crude was purified using flash chromatography (80g silica gel cartridge, hexane ethyl acetate (0-20% EtOAc). 1.2 g of compound **8** was obtained with 63% yield. ^{1}H NMR (600 MHz, chlorophorm-d) δ 10.41 (s, 1H), 7.86 (d, *J* = 8.8 Hz, 1H), 7.26 (s, 1H), 7.24 (d, *J* = 8.8 Hz, 1H), 4.86 (br. s., 1H), 4.48 (s, 2H), 2.88 (s, 3H), 1.94 (s, 6H), 1.39 (s, 9H); ^{13}C NMR (151 MHz, CHLOROFORM-d) δ 191.2, 154.6, 139.5, 137.8, 127.7, 127.7, 127.3, 113.3, 112.8, 111.0, 108.5, 79.8, 52.7, 45.9, 45.7, 36.4, 28.3, 14.5

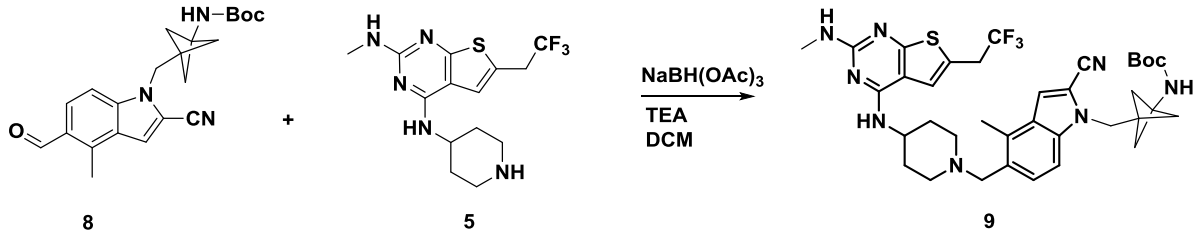

8 5 9

***tert*-butyl (3-((2-cyano-4-methyl-5-((4-((2-(methylamino)-6-(2,2,2-trifluoroethyl)thieno[2,3-d]pyrimidin-4-yl)amino)piperidin-1-yl)methyl)-1H-indol-1-yl)methyl)bicyclo[1.1.1]pentan-1-yl)carbamate (9)** Compouond **5** (2.1 g, 6 mmol, 1.0 eq) was suspended in DCM (60 mL) and aldehyde **8** (2.4g, 6.3 mmol, 1.1 eq) was added followed by TEA (3.3 mL, 24 mmol, 4 eq). The reaction mixture was stirred for 30 min at room temperature. Sodium triacetoxyborohydride (2.8 g, 13.2 mmol, 2.2 eq) was added and the mixture was stirred at rt overnight. The reaction mixture was diluted with DCM:MeOH (10:1, *v/v*) and the organic phase was washed with 1M NaOH (2x50 mL), brine and dried over sodium sulfate. Solvent was removed and the residue was purified using flash chromatography (hexane:EtOAc, to wash remaining aldehyde **8**, then DCM:MeOH (with 5% NH_4OH_{aq} 5%), gradient 0-15% for 20 min) to afford 3.4 g of

compound **9** (80% yield).[1]H NMR (600 MHz, chloroform-d) δ 7.32 (d, *J* = 8.8 Hz, 1H), 7.19 (s, 1H), 7.09 (d, *J* = 8.4 Hz, 1H), 6.82 (s, 1H), 4.88 (br. s., 1H), 4.82 (q, *J* = 5.1Hz, 1H), 4.73 (d, *J* = 7.7 Hz, 1H), 4.43 (s, 2H), 4.07 - 4.13 (m, 1H), 3.59 (s, 2H), 3.52 (q, *J* = 10.0 Hz, 2H), 3.00 (d, *J* = 5.1 Hz, 3H), 2.87 (d, *J* = 12.1 Hz, 2H), 2.55 (s, 3H), 2.23 (t, *J* = 10.6 Hz, 2H), 2.05 - 2.12 (m, 2H), 1.94 (s, 6H), 1.48 - 1.60 (m, 2H), 1.40 (s, 9H); [13]C NMR (151 MHz, chloroform-d) d 171.1, 169.7, 160.8, 156.5, 154.8, 136.7, 131.0, 129.0, 127.2, 124.9 (*J* = 278.40 Hz), 120.7, 118.4, 113.8, 111.8, 109.5, 109.1, 107.3, 79.7, 60.3, 52.8, 52.4, 47.8, 45.7, 45.6, 36.6, 35.5, 32.5, 28.6, 28.3, 15.0. HR-MS m/z calculated for [M+H$^+$]: 709.3255 found: 709.3264

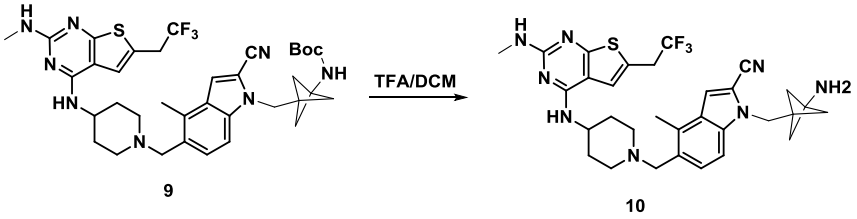

9 10

1-((3-aminobicyclo[1.1.1]pentan-1-yl)methyl)-4-methyl-5-((4-((2-(methylamino)-6-(2,2,2-trifluoroethyl)thieno[2,3-d]pyrimidin-4-yl)amino)piperidin-1-yl)methyl)-1H-indole-2-carbonitrile (10) Compound **9** (3.3 g, 4.7 mmol) was suspended in 22 mL of DCM 22 ml and 7.2 mL of TFA was added slowly. The reaction mixture was stirred for 2h until no starting material was present in the mixture. Volatiles were evaporated, and the residue was suspended in 200 mL of DCM 200 mL and poured into ice-cold concentrated aqueous solution of ammonia (pH>12). The aqueous phase was extracted with DCM:MeOH (10:1, 2x75ml) and the combined organic phases were dried over sodium sulfate and concentrated. The crude product was used to a next step without further purification (2.5g, 89% yield). [1]H NMR (600 MHz, chloroform-d) δ 7.33 (d, *J* = 8.44 Hz, 1H), 7.19 (s, 1H), 7.10 (d, *J* = 8.44 Hz, 1H), 6.82 (s, 1H), 4.78 - 4.87 (m, 1H), 4.72 (d, *J* = 7.70 Hz, 1H), 4.40 (s, 2H), 4.06 - 4.19 (m, 1H), 3.59 (s, 2H), 3.52 (q, *J* = 10.03 Hz, 2H), 3.00 (d, *J* = 4.77 Hz, 3H), 2.81 - 2.92 (m, 2H), 2.56 (s, 3H), 2.19 - 2.27 (m, 2H), 2.03 - 2.11 (m, 2H), 1.73 (s, 6H), 1.63 (br. s., 3H), 1.48 - 1.59 (m, 2H); [13]C NMR (151 MHz, chloroform-d) δ 169.7, 160.8, 156.4, 136.7, 130.9, 128.8, 128.8, 127.2, 124.9 (J = 277.3 Hz), 120.7, 118.4, 113.8, 111.6, 109.5, 109.1, 107.3, 60.3, 53.5, 52.4, 49.1, 47.8, 45.9, 35.4 (J = 31.9 Hz), 34.2, 32.5, 28.5, 15.0; LC-MS [M+H$^+$]: 609

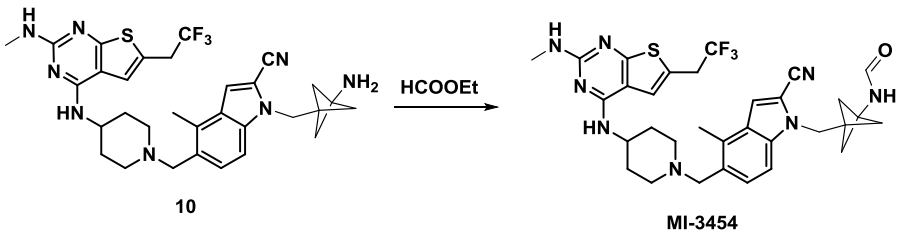

10 MI-3454

N-(3-((2-cyano-4-methyl-5-((4-((2-(methylamino)-6-(2,2,2-trifluoroethyl)thieno[2,3-d]pyrimidin-4-yl)amino)piperidin-1-yl)methyl)-1H-indol-1-yl)methyl)bicyclo[1.1.1]pentan-1-yl)formamide (MI-3454). Compound **10** (2.49 g, 4.1 mmol) and DMAP (100 mg, 0.8 mmol, 0.2 eq) were suspended in ethyl formate (14 mL) and refluxed for 48 h until only traces of starting material were present in the mixture. Ethyl formate was evaporated and residue was dissolved in DCM:MeOH (10:1, *v/v*, 150 mL) and washed with 1M NaOH (2x45 mL). The separated organic phase was dried over sodium sulfate and concentrated. The crude material was loaded on silica gel cartridge (80g) and purified using DCM:MeOH (with 5%NH_4OH) gradient 0% to 15% MeOH (with 5%$_{vol}$ ammonia). The eluent was concentrated to provide a sticky solid. Repeated DCM addition and evaporation converted the oily residue to a fine, loose solid. The solid was dissolved in EtOH at 45 ^oC and water was added to precipitate the product. The suspension was cooled at 0 ^oC for 4h and filtered off. The obtained solid was washed with MiliQ water and lyophilized to provide 2.1 g of white powder (81%); ^1H NMR (600 MHz, chloroform-d) δ 8.05 (s, 0.5H)*, 8.02 (d, *J* = 11.7 Hz, 0.5H)*, 7.36 (d, *J* = 8.4 Hz, 0.5H)*, 7.33 (d, *J* = 8.4 Hz, 0.5H)*, 7.22 (s, 0.5H)*, 7.20 (s, 0.5H)*, 7.09 (d, *J* = 8.4 Hz, 1H), 6.83 (s, 1H), 6.04 (d, *J* = 11.7 Hz, 0.5H)*, 5.78 (br. s., 0.5H)*, 4.80 - 4.88 (m, 1H), 4.68 - 4.80 (m, 1H), 4.47 (s, 1H)*, 4.44 (s, 1H)*, 4.08 - 4.18 (m, 1H), 3.59 (m, 2H), 3.52 (q, *J* = 10.2 Hz, 2H), 3.00 (d, *J* = 4.8 Hz, 3H), 2.81 - 2.92 (m, 2H), 2.54 - 2.60 (m, 3H), 2.17 - 2.29 (m, 2H), 2.05 - 2.11 (m, 2H), 2.01 (s, 3H)* 1.98 (s, 3H)*, 1.46 - 1.59 (m, 2H); *distinguishable rotamers signals; ^{13}C NMR (151 MHz, chloroform-d) δ 169.7, 162.7, 160.9, 160.8, 156.5, 136.7, 136.6, 131.2, 131.0, 129.2, 129.1, 129.0, 129.0, 127.3, 127.2, 124.9 (*J* = 277.3Hz), 120.6, 118.4, 118.4, 113.7, 113.7, 112.1, 111.9, 109.5, 109.0, 107.1, 106.9, 60.3, 53.2, 53.1, 52.4, 47.8, 45.8, 45.4, 45.1, 45.0, 37.3, 36.3, 35.4 (*J* = 31.9Hz), 32.5, 28.5, 15.0, 14.9; ^{19}F NMR (376 MHz, $CDCl_3$) δ -66.4 (t, *J* = 10.9 Hz); HR-MS m/z calculated for [$M+H^+$]: 637.2679 found: 637.2680;

Supplementary References

1. Borkin D, et al. Pharmacologic inhibition of the Menin-MLL interaction blocks progression of MLL leukemia in vivo. *Cancer Cell.* 2015;27(4):589-602.
2. Borkin D, et al. Property Focused Structure-Based Optimization of Small Molecule Inhibitors of the Protein-Protein Interaction between Menin and Mixed Lineage Leukemia (MLL). *J Med Chem.* 2016;59(3):892-913.

3. Borkin D, et al. Complexity of Blocking Bivalent Protein-Protein Interactions: Development of a Highly Potent Inhibitor of the Menin-Mixed-Lineage Leukemia Interaction. *J Med Chem.* 2018;61(11):4832-50.

4. Otwinowski Z, and Minor W. *Macromolecular Crystallography, Pt A*. 1997:307-26.

5. Murshudov GN, Vagin AA, and Dodson EJ. Refinement of macromolecular structures by the maximum-likelihood method. *Acta Crystallogr D Biol Crystallogr.* 1997;53(Pt 3):240-55.

6. Emsley P, and Cowtan K. Coot: model-building tools for molecular graphics. *Acta Crystallogr D Biol Crystallogr.* 2004;60(Pt 12 Pt 1):2126-32.

7. The CCP4 suite: programs for protein crystallography. *Acta Crystallogr D Biol Crystallogr.* 1994;50(Pt 5):760-3.

8. Adams PD, et al. PHENIX: a comprehensive Python-based system for macromolecular structure solution. *Acta Crystallogr D Biol Crystallogr.* 2010;66(Pt 2):213-21.

9. Davis IW, et al. MolProbity: all-atom contacts and structure validation for proteins and nucleic acids. *Nucleic Acids Res.* 2007;35(Web Server issue):W375-83.

10. Yang H, Guranovic V, Dutta S, Feng Z, Berman HM, and Westbrook JD. Automated and accurate deposition of structures solved by X-ray diffraction to the Protein Data Bank. *Acta Crystallogr D Biol Crystallogr.* 2004;60(Pt 10):1833-9.